# COX-2 inhibition combined with radiation reduces orthotopic glioma outgrowth by targeting the tumor vasculature.

Wagemakers, Michiel; van der Wal, Gesiena E.; Cuberes, Rosa; Alvarez, Ines; Ma Andres, Eva; Buxens, Jordi; Vela, Jose M.; Moorlag, Henk; Mooij, Jan Jakob A.; Molema, Grietje

*Published in:*
Translational oncology

*DOI:*
10.1593/tlo.08160



*Publication date:*
2009

Translational Oncology
www.transonc.com

Volume 2 Number 1 March 2009 pp. 1–7 1

# COX-2 Inhibition Combined with Radiation Reduces Orthotopic Glioma Outgrowth by Targeting the Tumor Vasculature[1]

**Michiel Wagemakers*,[2], Gesiena E. van der Wal[†,2], Rosa Cuberes[‡], Inés Álvarez[‡], Eva M[a] Andrés[‡], Jordi Buxens[‡], José M. Vela[‡], Henk Moorlag[†], Jan Jakob A. Mooij* and Grietje Molema[†]**

*Department of Neurosurgery, University Medical Center Groningen, University of Groningen, Groningen, The Netherlands; [†]Department of Pathology and Laboratory Medicine, Medical Biology section, University Medical Center Groningen, University of Groningen, Groningen, The Netherlands; [‡]Laboratorios ESTEVE, Barcelona, Spain

## Abstract

Cyclooxygenase 2 (COX-2) inhibitors have been shown to enhance tumor's response to radiation in several animal models. The strong association of COX-2 and angiogenesis suggests that the tumor vasculature may be involved in this process. The current study investigated whether treatment with the COX-2 inhibitor E-6087 could influence response to local radiation in orthotopically growing murine gliomas and aimed to analyze the involvement of the tumor vasculature. GL261 glioma cells were injected into the cerebrum of C57bl/6 mice. From day 7 after tumor cell injection, mice were treated with COX-2 inhibitor at 50 mg/kg i.p. every third day. Radiation consisted of three fractions of 2 Gy given daily from day 9 to day 11. Mice were killed at day 21. The COX-2 inhibitor significantly enhanced the response to radiation, reducing mean volume to 32% of tumors treated with radiation only. The combination treatment neither increased apoptosis of tumor cells or stromal cells nor affected tumor microvascular density. *In vitro*, E-6087 and its active metabolite did not affect clonogenic survival of GL261 cells or human umbilical vein endothelial cell after radiation. *In vivo*, however, there was a nonsignificant increase in Angiopoietin (Ang)-1 and Tie-2 mRNA levels and a decrease of Ang-2 mRNA levels after combination treatment. These changes coincided with a significant increase in α-smooth muscle actin–positive pericyte coverage of tumor vessels. In conclusion, the antitumor effect of radiation on murine intracranial glioma growth is augmented by combining with COX-2 inhibition. Our findings suggest an involvement of the tumor vasculature in the observed effects.

*Translational Oncology (2009) 2, 1–7*

## Introduction

The growth of solid tumors depends on the formation of new vessels from preexisting ones, or angiogenesis. In angiogenesis research, gliomas have received special attention because of their high vascular density. Cyclooxygenase 2 (COX-2), an inducible prostaglandin synthetase, is strongly associated with tumor angiogenesis [1]. It is overexpressed in gliomas and in other tumors, and its expression is correlated with vascular density and prognosis [2,3]. Inhibition of COX-2 resulted in a reduction of angiogenesis [4] and in a reduction of glioma growth [5].

COX-inhibitors have been shown to exert a synergistic antitumor effect in combination with radiation treatment in several tumors *in vivo* [6–10]. Some controversy exists about the molecular and cellular basis for this synergy. The ability of COX-2 inhibitors to suppress neovascularization suggests that mechanisms related to tumor vascular function may be involved in the radiosensitizing effects of these drugs [11].

The aim of our research, therefore, was to analyze the effects of the combination of a COX-2 inhibitor with radiotherapy on gliomas

Address all correspondence to: Michiel Wagemakers, Department of Neurosurgery, University Medical Center Groningen, PO Box 30.001, 9700 RB Groningen, the Netherlands. E-mail: m.wagemakers@nchir.umcg.nl

[1]This work was supported in part by grants from the Dutch Cancer Society (to M.W., J.J.A.M., and G.M.), Jan Kornelis de Cock Foundation (to M.W.), and Junior Scientific Masterclass Studentship (to G.W.).

[2]These authors contributed equally to this work.

Received 4 August 2008; Revised 30 September 2008; Accepted 1 October 2008



1944-7124 DOI 10.1593/tlo.08160

*in cerebro* and to investigate to what extent the tumor vasculature is involved in the therapeutic response. We used a model that uses orthotopically implanted syngeneic GL261 glioma cells in C57bl/6 mice. In this model, invasive growth and neovascularization have been extensively described [12,13].

We here demonstrate a reduced outgrowth of intracranial glioma caused by the systemic addition of a COX-2 inhibitor to local fractionated radiation and find indications for the involvement of the tumor vasculature in the observed antitumor effects.

## Materials and Methods

### *COX-1 and COX-2 Inhibitory Effects*

The effect of E-6087 (see Figure 1 for chemical structure) on COX-1 and COX-2 enzymatic activity was assessed according to a modification of the method described by Takeguchi and Sih [14]. *In vivo*, E-6087 is metabolized into another active compound, E-6132 (Figure 1), which was analyzed for its effect on COX-1 and -2 activity in the same way. For comparison, the effect of celecoxib was assessed in parallel.

*In vivo*, prostaglandin $E_2$ ($PGE_2$) production inhibition was determined in a rat inflammatory exudate (COX-2) and gastric mucosa (COX-1) model, as previously described [15]. The $PGE_2$ generation was determined by enzyme immunoassay using an immunoassay detection kit (Cayman Chemical Co., Ann Arbor, MI; Catalog no. 5140) according to the manufacturer's instructions.

E-6087 and E-6132 have been synthesized at the Chemistry Department of Laboratorios Esteve (Barcelona, Spain).

### *Cells*

Human umbilical vein endothelial cells (HUVECs) were obtained from the Endothelial Cell Facility UMCG (Groningen, the Netherlands). Cells were isolated and cultured as previously described [16].

GL261 murine glioma cells, kindly provided by Dr. U Herrlinger (Hertie Institute for Clinical Brain Research, Tubingen, Germany), were cultured in tissue culture flasks at 37°C under 5% $CO_2$–95% air. The GL261 culture medium consisted of Dulbecco's modified Eagle's medium supplemented with 10% FCS, 2 mM L-glutamine, and 1% gentamicin (Biowittaker, Verviers, Belgium). All experiments were performed with confluent GL261 monolayers, except for the clonogenic survival assays, in which confluency status was as described below.

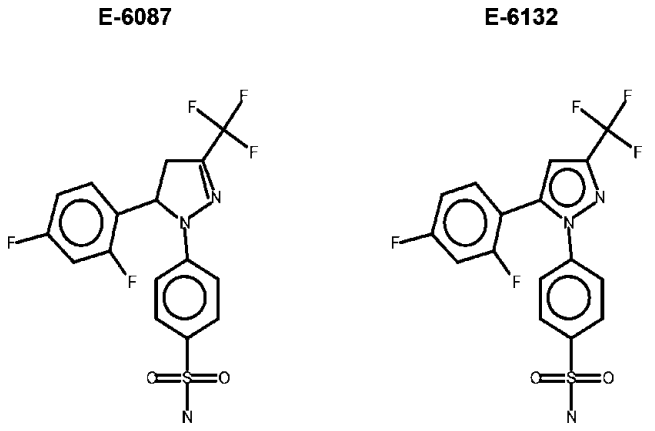


**Figure 1.** Chemical structures of E-6087 and its metabolite E-6132. E-6087 (a crystalline solid with a molecular weight of 405.35) is an inhibitor of cyclo-oxygenase with preferential effects on COX-2. *In vivo*, it is metabolized into the even more potent COX-2 inhibitor E-6132, with plasma concentrations of the metabolite in rats being lower than those of the parental compound. Pharmacokinetics studies of E-6087 in rats and dogs [29] showed peak plasma concentrations 2 to 7 hours after oral administration. Elimination $t_{1/2}$ was 15 to 34 hours with a plasma clearance of 0.1 to 0.22 L/h per kilogram. These parameters varied with species and gender.

### *Animals*

Immunocompetent male C57bl/6 mice were purchased from Harlan (Horst, the Netherlands). Animals were maintained on mouse chow and acidified tap water *ad libitum* in a temperature-controlled chamber at 24°C with a 12-hour light/dark cycle. The mice were monitored daily for behavior and every other day for body weight. All experiments were approved by the local ethics committee on animal research and were performed in accordance with the Dutch Code of Practice for animal experiments in oncological research.

### *Animal Experimental Procedures*

GL261 murine glioma cells, which are syngeneic to C57bl/6 mice, were orthotopically implanted. This model was chosen for its known invasive properties [13] and its well-documented induction of neoangiogenesis [12]. Implantation of GL261 cells into the brains of C57bl/6 mice was performed under anesthesia. All procedures requiring anesthesia were performed using ketamine (75 mg/kg) and medetomidine (1 mg/kg) i.p. Animals recovered from anesthesia after i.m. injection with Antisedan (0.6 mg/kg). Additionally, for analgesia during tumor cell implantations, Rimadyl (5 mg/kg) was administered s.c.

Three microliters of tumor cell suspension (100,000 cells/μl) was stereotactically inoculated in the left striate nucleus using a 10-μl SGE syringe (SGE Scientific, Melbourne, Australia).

On day 7 after tumor cell inoculation, mice were randomly assigned to treatment groups. Mice were i.p. injected with COX-2 inhibitor E-6087 (50 mg/kg) suspended in 5% gum arabic (15 mg/ml) every third day, until the end of the experiment (day 21). Control mice received injections with vehicle only. Local radiation in three fractions was started at day 9, for 3 consecutive days, one fraction of 2 Gy/day (1.8 Gy/min) to a total of 6 Gy. Mice were radiated using a MGC 41 X-ray machine (Yxlon International, Hamburg, Germany; 200 kV, 10 mA). The animals were anesthetized and positioned under a leaden shield (thickness >3 mm). Radiation was performed through a 1 × 0.8-cm rectangular hole in the shield that was positioned over the left cerebral hemisphere. Tumor-bearing control mice were sham-radiated.

On day 21, mice were anesthetized, and the brains were removed under perfusion with sterile 0.9% NaCl. The brains were snap frozen in isopentane and stored at −80°C.

### *Tumor Volume Measurements*

For tumor volume measurements, mouse brains were mounted on a cryostat (CM 1900; Leica, Wetzlar, Germany), and the cutting of 5-μm cryosections was started at the rostral end. Tumor volumes

were calculated from surface area measurements of every 20th tissue section of the tumor.

### *Clonogenic Survival Assay*

Human umbilical vein endothelial cells (first passage) and GL261 (up to passage 40) were plated in 25-$cm^2$ gelatin-coated culture flasks in increasing densities (ranging from 100 to 100,000 cells per flask). Twenty-four hours after plating, cells were radiated with graded doses (0, 3, 5, or 10 Gy) with a Cs-137 γ-ray machine (dose rate: 0.765 Gy/min). Two hours before radiation, cells were incubated with either E-6087 or E-6132 in a concentration of 10 μM or vehicle only in EC medium. Feeder cells consisted of HUVEC or GL261 cells radiated with a lethal dose of 100 Gy (100,000 cells per flask, added before radiation; dose rate: 2.226 Gy/min). Half of the medium was refreshed for the first time after 8 days. After 14 days, cultures were gently washed with phosphate-buffered saline, and colonies were stained with crystal violet 1% (Sigma, St. Louis, MO) in ethanol 30%–formaldehyde 3% in demineralized water. Colonies containing more than 50 cells were counted. A minimum of two independent experiments were performed per experimental setup.

### *Immunohistochemistry*

Cryostat sections were immunohistochemically analyzed using standard protocols. The primary antibodies used recognized CD31 (Catalog no. 55027; BD Biosciences-PharMingen, San Diego, CA), caspase 3a (Catalog no. 557035; BD Biosciences-PharMingen), COX2 (Catalog no. ab21704; Abcam, Cambridge, UK), CD45 (Catalog no. 550539; BD Biosciences-PharMingen).

Similarly, fluorescence double staining was performed using standard protocols. The primary antibodies used recognized CD31, desmin (Catalog no. ab152001; Abcam), and α-smooth muscle actin (αSMA; Cy3-labeled, Catalog no. C6198; Sigma-Aldrich).

### *Determination of Tumor Microvascular Density*

Microvascular density (MVD) was scored using the Chalkley point overlap morphometric technique, which allows for rapid analysis with a relatively low interobserver variability [17]. This method has been described in detail [18]. In brief, three vascular hot spots were identified per tumor. A 25-point Chalkley eyepiece graticule (Graticules Ltd, Edenbridge, Kent, UK) was used to score each hot spot at a magnification of ×200. The graticule was oriented to permit the maximum number of points to hit the immunohistochemically visualized microvessels. This procedure was performed in duplicate. The MVD per tumor was obtained by calculating the mean of these three hot spots. Results were confirmed by the independent analysis of a second observer.

### *Analysis of Pericyte Coverage of Tumor Vessels*

Cryosections were double stained for CD31 and αSMA or desmin. Per tumor, six or more random high-power fields were analyzed on a fluorescence microscope (Quantimed 600S; Leica Camera, Solms, Germany) equipped with a 40× objective lens (Leica PL Fluotar). Using the appropriate filters, images were captured with the Leica QWin 3 software. All vessels within the high-power field were analyzed. A minimum of 30 vessels per tumor were scored. The percentage of vessels that showed any perivascular staining for αSMA or desmin was scored. Results were confirmed by the independent analysis of a second observer.

### *Gene Expression Analysis by Real-time Reverse Transcription–Polymerase Chain Reaction*

Total RNA was isolated with Absolutely RNA Micropep Kit (Stratagene, Amsterdam, the Netherlands) according to the protocol of the manufacturer.

RNA was analyzed qualitatively by gel electrophoresis and quantitatively using Nanodrop (Nanodrop Technologies, Rockland, DE). One microgram of total cellular RNA was subsequently used for the synthesis of first-strand cDNA with SuperScript III RNase H minus reverse transcriptase (Invitrogen, Breda, the Netherlands) in a 20-μl final volume containing 250 ng of random hexamers (Promega, Benelux, Leiden, the Netherlands) and 40 U of RNase OUT inhibitor (Invitrogen). After the RT reaction, 1 μl of cDNA was used for each PCR. Exons overlapping primers and minor groove binder probes used for real-time reverse transcription–polymerase chain reaction (RT-PCR) were purchased as Assay-on-Demand from Applied Biosystems (Nieuwekerk a/d IJssel, the Netherlands). As a control, water was analyzed to exclude unspecific signals arising from impurities and consistently showed no amplification signals. *Taq*Man PCR was performed as previously described [16].

### *Statistical Analysis*

Statistical significance of differences was tested with GraphPad Prism 3 (GraphPad Software, La Jolla, CA) using the one-way analysis of variance assuming normal distribution of the data. The differences were considered significant at $P < .05$.

## Results

### *E-6087 and E-6132 Are Potent and Selective Inhibitors of COX-2* In Vitro *and* In Vivo

Both E-6087 and E-6132 were potent inhibitors of the COX-2 enzymatic activity. E-6087 was more than 100-fold selective for COX-2 *versus* COX-1 [$IC_{50}$ (μM): *COX-1*, 334 (95% confidence interval (CI), 226-442); and *COX-2*, 2.93 (95% CI, 2.03-3.83)]. In the case of its main metabolite, the selectivity for COX-2 over COX-1 was >250-fold [$IC_{50}$ (μM): *COX-1*, 134 (95% CI, 10-259); and *COX-2*, 0.5 (95% CI, 0.11-0.88)]. For comparison, the selectivity of celecoxib was >300-fold [$IC_{50}$ (μM): *COX-1*, 90.2 (95% CI, 73.5-106.7); and *COX-2*, 0.28 (95% CI, 0.15-0.41)]. E-6087 and E-6132 potently inhibited the production of $PGE_2$ in rat carrageenan-induced inflammatory exudates, with per os (p.o.) $ED_{50}$ for E-6087 of 7.38 mg/kg (SEM 1.3) and for E-6132 1.8 mg/kg (SEM 0.2). The $ED_{50}$ for celecoxib was 2.85 mg/kg (SEM 0.61). In contrast, no significant inhibition of $PGE_2$ production was observed in gastric mucosa samples even when the compounds were administered at the highest dose tested (40 mg/kg, p.o. for E-6087 and E-6132; 20 mg/kg for celecoxib).

### *Combination of COX-2 Inhibition and Radiation Therapy Resulted in a Significant Additive Reduction in Glioma Outgrowth*

We initiated intracerebral tumors in 28 mice and randomly assigned mice to one of four study groups ($n = 7$). One mouse died before the end of the experiment. Its death was unrelated to tumor growth, administration of COX-2 inhibitor, or radiation treatment. Two more mice (one from the COX-2 inhibitor group and one from the combination group) did not grow any identifiable tumor and

were excluded from the study. As such a take rate 93% was established. After exclusion of these three mice, three groups of six mice each and one group of seven mice (radiation group) remained. Mean tumor volume of the untreated group was the largest of all four groups (52.7 $mm^3$, SD 11.2), differing significantly from the radiation group ($P < .001$) with mean tumor volume of 22.4 $mm^3$ (SD 12.1; Figure 2). The mean tumor volume of the group treated with the combination of COX-2 inhibitor and fractionated radiation was the lowest of all groups: 7.1 $mm^3$ (SD 4.6). Besides a difference with the untreated group ($P < .001$), this volume was significantly smaller than the mean tumor volume of the group treated with radiation only ($P < .05$). The variance in the group treated with COX-2 inhibitor only (mean tumor volume, 25.7 $mm^3$ (SD 27.9)) was such that no significant difference was found with the other groups (combination *vs* COX-2 inhibitor alone; $P = .14$). Representative microscopic images of tumors from the four treatment groups are shown in Figure 3. They illustrate the dramatic differences between the groups at the end of the experiment, varying from dense compact tumors in the control group to disintegrated tumors in the combination group.

### *Tumor Cells Are Not Targeted by the COX-2 Inhibitor*

To investigate whether the tumor cells could present as a possible target of COX-2 inhibition, we analyzed COX-2 mRNA expression in GL261 cells *in vitro* and *in vivo* by real-time RT-PCR. *In vitro*, no COX-2 mRNA was detected in the GL261 cell line. *In vivo*, *COX-2* gene expression was detectable in the tumors, which may be attributed to tumor stroma–associated cells, including endothelial cells and tumor-infiltrating leukocytes. Radiation did not affect the levels of COX-2 mRNA *in vitro* and *in vivo* (data not shown). However, immunohistochemistry showed more cells in the glioma tumor tissue staining positive for COX-2 in both the radiation-only group and in the combination treatment group. The distribution of COX-2–positive cells was consistent with the distribution of leukocytes as stained with CD45 (data not shown).

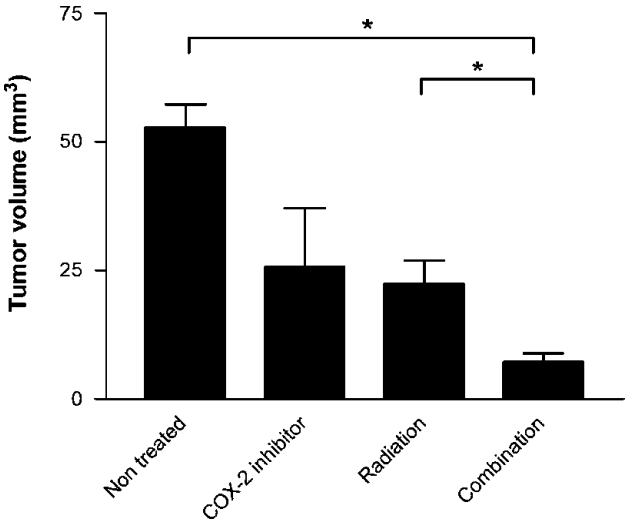


**Figure 2.** Antitumor effects of the COX-2 inhibitor E-6087 and local radiation in fractions on intracranial murine glioma growth. One week after tumor cell inoculation, mice were left untreated, treated with COX-2 inhibitor, treated with radiation, or treated with a combination of COX-2 inhibitor and radiation. (*) Combination therapy (mean tumor volume, 7.1 $mm^3$) significantly reduced tumor outgrowth compared with radiation-only (mean tumor volume, 22.4 $mm^3$; $P < .05$) and compared with nontreated tumors (mean tumor volume, 52.7 $mm^3$; $P < .001$). Mean tumor volume of mice treated with COX-2 inhibitor was 25.7 $mm^3$. The mean volume per group is presented, $n = 6$, except for the radiation group for which $n = 7$, ± SEM.

Because a COX-2–negative state of the tumor cells does not exclude COX-2–independent inhibiting effects on tumor cells [19], we next analyzed tumor cell apoptosis. Active caspase 3 (caspase 3a) staining was virtually absent in the untreated group and in the mice treated with COX-2 inhibitor only. Variable amounts of caspase 3a–positive cells were detected in the radiation group and in the mice treated with COX-2 inhibitor plus radiation. The distribution of the apoptotic cells, however, colocalized with the distribution of the infiltrating leukocytes as identified by CD45 immunohistochemical staining, suggesting that the therapeutic strategies used here induced cell death in the host-derived tumor-infiltrating leukocytes.

In the absence of induction of apoptosis, a change in clonogenic survival may explain alteration of the tumor's response to radiation. In the clonogenic survival assay, however, no significant effects of E-6087 on survival after radiation could be detected. To exclude the possibility of an actual clonogenic cell death–inducing effect by the active metabolite E-6132, which is formed *in vivo* from E-6087, we repeated the experiment with this metabolite. Although E-6132 did reduce clonogenic survival in tumor cells, the extent of reduction was constant regardless of radiation dosage and was statistically not significant (data not shown).

### *Tumor Vasculature as a Possible Target for COX-2 Inhibition Plus Radiation Therapy*

As described above, increased apoptosis was observed in the tumor-infiltrating leukocytes after combination therapy. An immunofluorescence double staining procedure was not able to colocalize tumor endothelial cells, as identified by CD31 (PECAM-1) staining and caspase 3a positivity (data not shown).

If the additional antitumor effect of the combination treatment were to be related to the destruction of tumor vessels during the treatment period, this vascular effect may be represented by a change in MVD. The Chalkley point grid analyses of CD31-stained tumor vessels, however, demonstrated that the MVD was similar in all four groups. Because a vascular effect cannot be unambiguously excluded based on MVD data, we analyzed *in vitro* whether COX-2 inhibition affected radiation-induced clonogenic cell survival of HUVEC. Yet, both E-6087 and its active metabolite E-6132 neither significantly attenuated nor enhanced clonogenic cell survival in these cells (data not shown).

### *Combination Therapy Leads to Changes in the Tumor Vasculature Which Identifies the Vasculature as Target for Therapy*

The absence of an apoptosis- or clonogenic death–inducing effect on endothelial cells and the absence of a change in MVD do not *a priori* exclude the occurrence of a change in angiogenic potential as a result of combination treatment. We therefore studied the effects of the combination treatment on the expression levels of vascular endothelial growth factor (VEGF), the Ang/Tie-2 system, and other angiogenesis-related genes by real-time RT-PCR analysis ($n = 3$).

As an indication of the biologic activity of E-6087, we observed an increase in COX-2 mRNA in animals treated with COX-2 inhibitor

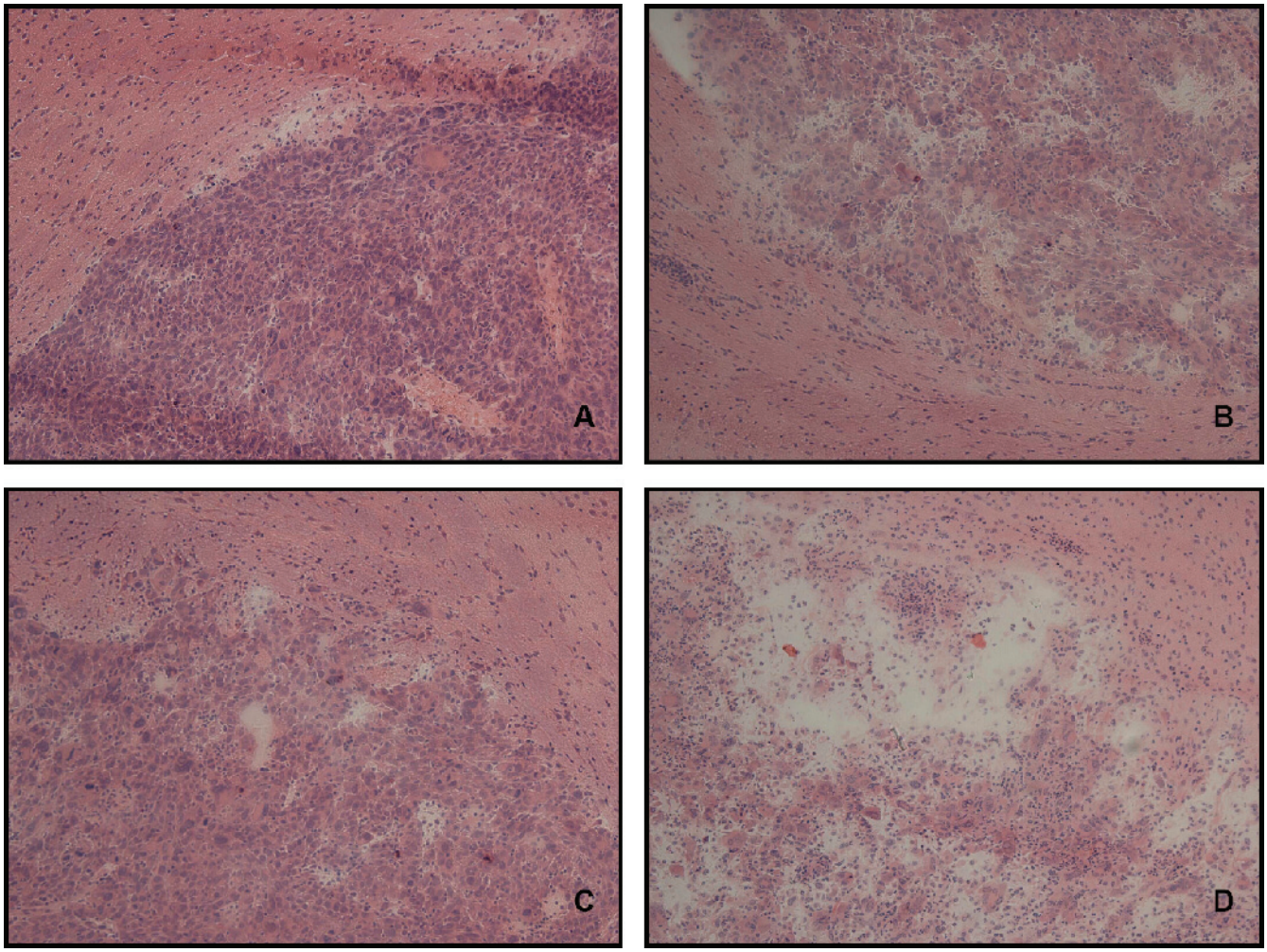


**Figure 3.** Combination therapy for COX-2 inhibition and radiation reduced tumor cell density and led to an apparent disintegration of the tumor. Representative cryosections of tumors harvested at the end of the treatment period and stained with hematoxylin. Original magnification, ×100. (A) Nontreated tumor. (B) COX-2 inhibitor treatment (50 mg/kg every third day starting at day 7 after inoculation of tumor cells). (C) Fractionated radiation (three fractions of 2 Gy for 3 consecutive days starting at day 9). (D) Combination therapy for COX-2 inhibition and radiation. The tumors treated with a combination of COX-2 inhibition and radiation showed a clear decrease in tumor cell density with apparent cellular and stromal defects not seen to the same extent in other treatment groups.

and radiation (mRNA *vs* GAPDH of radiation *vs* combination treatment: $1.23 \times 10^{-5}$ *vs* $3.88 \times 10^{-5}$, $P < .05$; Figure 4). Using Western blot, a similar inducing effect, paralleled by a decrease in the COX-2 product $PGE_2$, was demonstrated by Kang et al. [10] after the incubation of U87MG cells with celecoxib. Both results are indicative of a positive feedback loop induced by the inhibition of COX-2 activity. The increase in COX-2 mRNA in our study coincided with nonsignificant increases in VEGFR-1, hypoxia-inducible factor 1α, and Tie-2. The mRNA levels of integrin $\alpha_v$ showed a decrease in animals treated with COX-2 inhibition and radiation compared with the nontreated group (mRNA *vs* GAPDH $15.4 \times 10^{-3}$ *vs* $10.7 \times 10^{-3}$, respectively, $P < .05$). However, the mRNA levels of integrin $\alpha_v$ did not show a significant difference between the radiation and the combination group. The mRNA levels of VEGF-A, VEGFR-2, VE-cadherin, integrin $\beta_3$, and CD31 were similar in all four treatment groups (data not shown). The group treated with COX-2 inhibition and radiation showed a statistically nonsignificant increase in the expression of Ang-1 (one-way analysis of variance, $P = .055$), whereas Ang-2 showed a nonsignificant decrease of gene expression ($P = .199$; Figure 5). In line with this, there was a nonsignificant increase in the Ang-1/Ang-2 ratio as a result of COX-2 inhibition and radiation ($P = .075$).

Shifts in the gene expression of the angiopoietin system can be expected to be found in case of changes in vessel maturation. Although the changes in gene expression of this system did not reach significance in this study, these changes prompted us to analyze an additional parameter of the maturation status of the tumor vasculature, which is the extent of coverage of the vasculature with pericytes. Staining for the pericyte markers αSMA and desmin showed a significant increase in αSMA-positive pericyte coverage of tumor vessels (Figure 5), corroborating the trends seen in mRNA analysis. Interestingly, staining for desmin was similar in all four groups.

## Discussion

In this study, we showed that the administration of the COX-2 inhibitor E-6087 in addition to radiation treatment increases the antitumor effect of the treatment on intracranial murine glioma growth compared with radiation only. The added effect of combination treatment was strong, reducing mean tumor volumes by almost

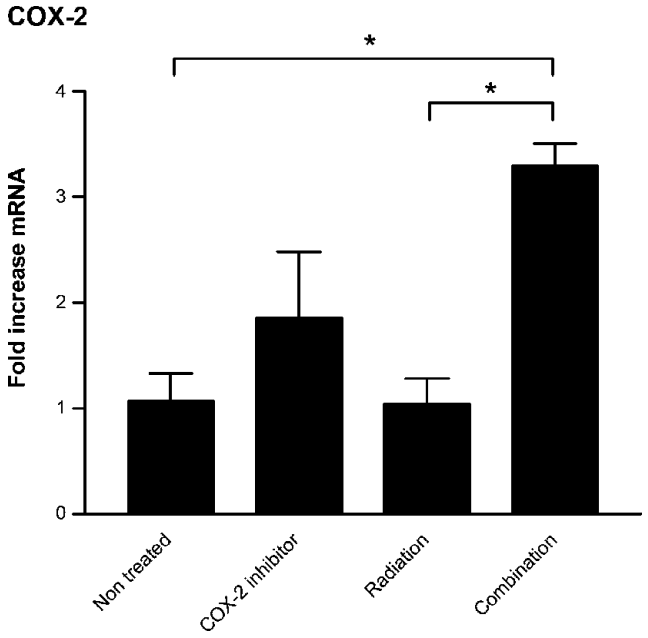


**Figure 4.** COX-2 inhibition induced an up-regulation of *COX-2* gene expression. Gene expression was analyzed with real-time RT-PCR. $C_T$ values were related to *GAPDH* gene expression. Gene expression is presented as fold increase in mRNA content normalized to the non treated control group. (*) The mean mRNA level of the mice treated with the combination of COX-2 inhibition and radiation was significantly increased compared to the control and radiation group, $P < .05$, $n = 3$, ± SEM.

70% compared with radiation treatment. The treatment did not affect tumor and endothelial cell proliferation and apoptosis. However, (neo)vascularization-related gene expression, but especially pericyte coverage of tumor vessels, may indicate that normalization of the tumor vasculature accompanied the reduced tumor growth.

The results presented here corroborate those of previous studies, which showed an enhancement of tumor radioresponse by COX inhibitors *in vivo* in several tumor types [6,7,20,21]. Kang et al. [10] recently confirmed the effect of combination treatment in an intracranial murine glioma model using U87 xenografts. Kang et al. showed a direct effect of this treatment on tumor cells *in vitro*. The absence of such an effect in our study may be explained by the fact that the GL261 cells used in our model do not express *COX-2 in vitro*. However, the growth inhibition of tumor cells by COX-2 inhibitors can occur in a COX-2–independent way [22,23]. Nonetheless, no effect of the combination treatment on the tumor cells was seen either *in vitro* or *in vivo*.

If the sensitization of radiation by COX-2 inhibition is not brought about by directly affecting the tumor cells then the tumor stroma must be involved.

Inhibition of angiogenesis may be of importance in the enhancement of radioresponsiveness induced by COX-2 inhibitors [24,25]. Masferrer et al. [1] demonstrated the antitumor effect of celecoxib in tumor models in which only the tumor endothelial cells were expressing *COX-2*. Kang et al. [10] demonstrated a reduction of MVD and changes in the gene expression levels of VEGF and the angiopoietin system after the combination treatment of radiation and celecoxib. We were not able to detect enhanced apoptosis or reduced clonogenic survival in endothelial cells after treatment with COX-2 inhibitors and radiation. Moreover, the MVD did not change as a response to treatment. The changes we found in the expression levels of the Ang/Tie-2 system, with an increase in the expression of Tie-2 and Ang-1, and a concomitant decrease in the expression of Ang-2, were all statistically nonsignificant. Nonetheless, this is in complete opposition with the decreased protein levels of VEGF and Ang-1, concomitant with an increased expression of Ang-2 in U87MG cells, found after radiation and incubation with celecoxib [10]. Several differences in study design may underlie these contradictory outcomes. First, Kang et al. measured the levels of the angiopoietin proteins in glioma cells *in vitro*. *In vivo*, however, the production of Ang-1 and Ang-2 relies on a number of different cell types, with the tumor cells or pericytes often accounting for Ang-1, and the endothelial cells for Ang-2 production. Second, in our study, we used real-time RT-PCR to measure gene expression, which neglects possible posttranscriptional regulation of two angiopoietin proteins. The results of the *Ang/Tie-2* gene expression analysis prompted us to analyze tumor vessel maturation and study whether

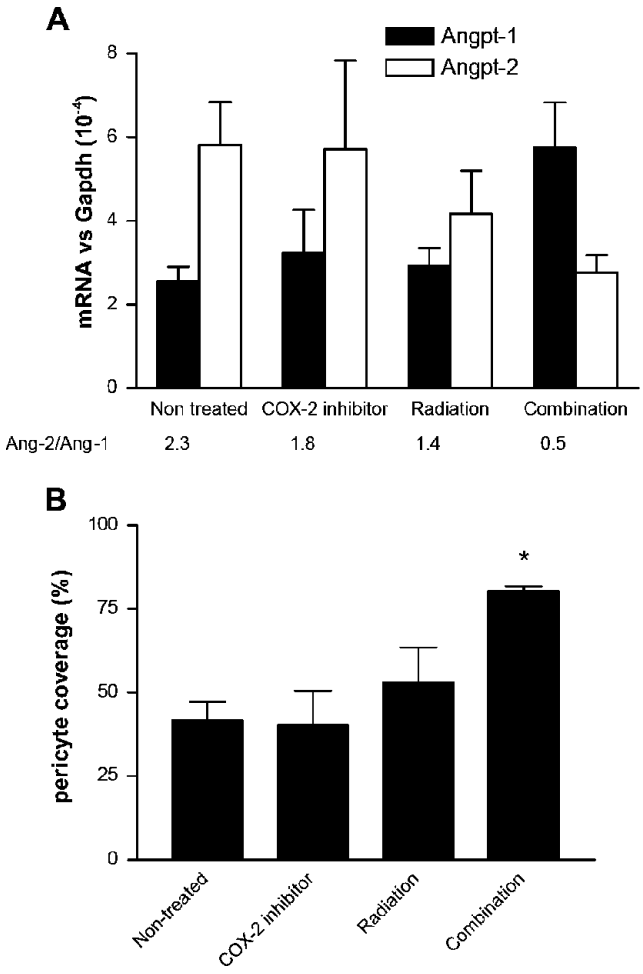


**Figure 5.** Changes in gene expression of Ang-1 and Ang-2 and pericyte coverage of tumor vessels are indicative of vessel normalization. (A) Ang-1 and Ang-2 gene expression in the different treatment conditions *versus* untreated controls. mRNA content was compared with *GAPDH*, $n = 3$, ± SEM. (B) αSMA-positive pericyte coverage of tumor vessels determined by CD31/αSMA double fluorescent immunostaining and subsequent quantification. (*) In response to treatment with a combination of E-6087 and radiation there is an increase in αSMA-positive pericyte coverage of tumor vessels compared to all other treatment groups, $P < .05$, $n = 3$, ± SEM.

vessel normalization had occurred. Vessel normalization is a process that counteracts changes in vascular behavior induced by the angiogenic process. It is hypothesized that tumor angiogenesis can be initiated only after a switch in the balance of Ang-1 and -2 in favor of the latter. It is the aim of vessel normalization therapy to reverse this switch. The clinical relevance and feasibility of vessel normalization have been illustrated in a clinical [26] and a preclinical setting [27]. Vessel normalization is associated with a recovery of pericyte coverage of the tumor vessels [28], a feature that was also seen in our current study. Because therapy in our model started relatively early, the suppressive effects of the treatment leading to vessel normalization possibly inhibited the ability of the tumor to induce an effective angiogenic switch and thereby inhibited tumor outgrowth.

In summary, we showed that COX-2 inhibition effectively inhibited GL261 intracranial glioma outgrowth when combined with radiation therapy. The changes in the tumor vasculature suggest a role for vessel normalization in the effects brought about. Further studies will be initiated to determine the molecular and cellular basis for the observed effects of the combination therapy. The strong effects warrant further studies on the feasibility of adding COX-2 inhibitor treatment to daily clinical practice in the treatment of high-grade glioma.

## Acknowledgments

The authors that the help of Peter Zwiers, Elise Langenkamp, and Ar Janssen for technical assistance during different analyses and Harry Kampinga for the clonogenic assay design.

## References

[1] Masferrer JL, Leahy KM, Koki AT, Zweifel BS, Settle SL, Woerner BM, Edwards DA, Flickinger AG, Moore RJ, and Seibert K (2000). Antiangiogenic and antitumor activities of cyclooxygenase-2 inhibitors. *Cancer Res* **60**, 1306–1311.

[2] Shono T, Tofilon PJ, Bruner JM, Owolabi O, and Lang FF (2001). Cyclooxygenase-2 expression in human gliomas: prognostic significance and molecular correlations. *Cancer Res* **61**, 4375–4381.

[3] Joki T, Heese O, Nikas DC, Bello L, Zhang J, Kraeft SK, Seyfried NT, Abe T, Chen LB, Carroll RS, et al. (2000). Expression of cyclooxygenase 2 (COX-2) in human glioma and *in vitro* inhibition by a specific COX-2 inhibitor, NS-398. *Cancer Res* **60**, 4926–4931.

[4] Leahy KM, Ornberg RL, Wang Y, Zweifel BS, Koki AT, and Masferrer JL (2002). Cyclooxygenase-2 inhibition by celecoxib reduces proliferation and induces apoptosis in angiogenic endothelial cells *in vivo*. *Cancer Res* **62**, 625–631.

[5] Matsuo M, Yoshida N, Zaitsu M, Ishii K, and Hamasaki Y (2004). Inhibition of human glioma cell growth by a PHS-2 inhibitor, NS398, and a prostaglandin E receptor subtype EP1-selective antagonist, SC51089. *J Neurooncol* **66**, 285–292.

[6] Petersen C, Petersen S, Milas L, Lang FF, and Tofilon PJ (2000). Enhancement of intrinsic tumor cell radiosensitivity induced by a selective cyclooxygenase-2 inhibitor. *Clin Cancer Res* **6**, 2513–2520.

[7] Kishi K, Petersen S, Petersen C, Hunter N, Mason K, Masferrer JL, Tofilon PJ, and Milas L (2000). Preferential enhancement of tumor radioresponse by a cyclooxygenase-2 inhibitor. *Cancer Res* **60**, 1326–1331.

[8] Milas L, Furuta Y, Hunter N, Nishiguchi I, and Runkel S (1990). Dependence of indomethacin-induced potentiation of murine tumor radioresponse on tumor host immunocompetence. *Cancer Res* **50**, 4473–4477.

[9] Furuta Y, Hunter N, Barkley T Jr, Hall E, and Milas L (1988). Increase in radioresponse of murine tumors by treatment with indomethacin. *Cancer Res* **48**, 3008–3013.

[10] Kang KB, Wang TT, Woon CT, Cheah ES, Moore XL, Zhu C, and Wong MC (2007). Enhancement of glioblastoma radioresponse by a selective COX-2 inhibitor celecoxib: inhibition of tumor angiogenesis with extensive tumor necrosis. *Int J Radiat Oncol Biol Phys* **67**, 888–896.

[11] Choy H and Milas L (2003). Enhancing radiotherapy with cyclooxygenase-2 enzyme inhibitors: a rational advance? *J Natl Cancer Inst* **95**, 1440–1452.

[12] Zagzag D, Amirnovin R, Greco MA, Yee H, Holash J, Wiegand SJ, Zabski S, Yancopoulos GD, and Grumet M (2000). Vascular apoptosis and involution in gliomas precede neovascularization: a novel concept for glioma growth and angiogenesis. *Lab Invest* **80**, 837–849.

[13] Zagzag D, Miller DC, Chiriboga L, Yee H, and Newcomb EW (2003). Green fluorescent protein immunohistochemistry as a novel experimental tool for the detection of glioma cell invasion *in vivo*. *Brain Pathol* **13**, 34–37.

[14] Takeguchi C and Sih CJ (1972). A rapid spectrophotometric assay for prostaglandin synthetase: application to the study of non-steroidal antiinflammatory agents. *Prostaglandins* **2**, 169–184.

[15] Tofanetti O, Casciarri I, Cipolla PV, Cazzulani P, and Omini C (1989). Effect of nimesulide on cyclo-oxygenase activity in rat gastric mucosa and inflammatory exsudate. *Med Sci Res* **17**, 745–746.

[16] Kuldo JM, Westra J, Asgeirsdottir SA, Kok RJ, Oosterhuis K, Rots MG, Schouten JP, Limburg PC, and Molema G (2005). Differential effects of NF-{kappa}B and p38 MAPK inhibitors and combinations thereof on TNF-{alpha}- and IL-1{beta}–induced proinflammatory status of endothelial cells *in vitro*. *Am J Physiol Cell Physiol* **289**, C1229–C1239.

[17] Vermeulen PB, Gasparini G, Fox SB, Colpaert C, Marson LP, Gion M, Belien JA, de Waal RM, Van ME, Magnani E, et al. (2002). Second international consensus on the methodology and criteria of evaluation of angiogenesis quantification in solid human tumours. *Eur J Cancer* **38**, 1564–1579.

[18] Fox SB, Leek RD, Weekes MP, Whitehouse RM, Gatter KC, and Harris AL (1995). Quantitation and prognostic value of breast cancer angiogenesis: comparison of microvessel density, chalkley count, and computer image analysis. *J Pathol* **177**, 275–283.

[19] Grosch S, Tegeder I, Niederberger E, Brautigam L, and Geisslinger G (2001). COX-2 independent induction of cell cycle arrest and apoptosis in colon cancer cells by the selective COX-2 inhibitor celecoxib. *FASEB J* **15**, 2742–2744.

[20] Nakata E, Mason KA, Hunter N, Husain A, Raju U, Liao Z, Ang KK, and Milas L (2004). Potentiation of tumor response to radiation or chemoradiation by selective cyclooxygenase-2 enzyme inhibitors. *Int J Radiat Oncol Biol Phys* **58**, 369–375.

[21] Pyo H, Choy H, Amorino GP, Kim JS, Cao Q, Hercules SK, and DuBois RN (2001). A selective cyclooxygenase-2 inhibitor, NS-398, enhances the effect of radiation *in vitro* and *in vivo* preferentially on the cells that express cyclooxygenase-2. *Clin Cancer Res* **7**, 2998–3005.

[22] Kuipers GK, Slotman BJ, Wedekind LE, Stoter TR, Berg J, Sminia P, and Lafleur MV (2007). Radiosensitization of human glioma cells by cyclooxygenase-2 (COX-2) inhibition: independent on COX-2 expression and dependent on the COX-2 inhibitor and sequence of administration. *Int J Radiat Biol* **83**, 677–685.

[23] Dittmann KH, Mayer C, Ohneseit PA, Raju U, Andratschke NH, Milas L, and Rodemann HP (2008). Celecoxib induced tumor cell radiosensitization by inhibiting radiation induced nuclear EGFR transport and DNA-repair: a COX-2 independent mechanism. *Int J Radiat Oncol Biol Phys* **70**, 203–212.

[24] Gately S and Li WW (2004). Multiple roles of COX-2 in tumor angiogenesis: a target for antiangiogenic therapy. *Semin Oncol* **31**, 2–11.

[25] Milas L, Kishi K, Hunter N, Mason K, Masferrer JL, and Tofilon PJ (1999). Enhancement of tumor response to gamma-radiation by an inhibitor of cyclooxygenase-2 enzyme. *J Natl Cancer Inst* **91**, 1501–1504.

[26] Hurwitz H, Fehrenbacher L, Novotny W, Cartwright T, Hainsworth J, Heim W, Berlin J, Baron A, Griffing S, Holmgren E, et al. (2004). Bevacizumab plus irinotecan, fluorouracil, and leucovorin for metastatic colorectal cancer. *N Engl J Med* **350**, 2335–2342.

[27] Winkler F, Kozin SV, Tong RT, Chae SS, Booth MF, Garkavtsev I, Xu L, Hicklin DJ, Fukumura D, di TE, et al. (2004). Kinetics of vascular normalization by VEGFR2 blockade governs brain tumor response to radiation: role of oxygenation, angiopoietin-1, and matrix metalloproteinases. *Cancer Cell* **6**, 553–563.

[28] Jain RK (2005). Normalization of tumor vasculature: an emerging concept in antiangiogenic therapy. *Science* **307**, 58–62.

[29] Reinoso RF, Farran R, Moragon T, Garcia-Soret A, and Martinez L (2001). Pharmacokinetics of E-6087, a new anti-inflammatory agent, in rats and dogs. *Biopharm Drug Dispos* **22**, 231–242.